International Communications in Heat and Mass Transfer 122 (2021) 105182

Contents lists available at ScienceDirect

International Communications in Heat and Mass Transfer

journal homepage: www.elsevier.com/locate/ichmt

The effects of external force and electrical field on the agglomeration of Fe_3O_4 nanoparticles in electroosmotic flows in microchannels using molecular dynamics simulation

Reza Balali Dehkordi [a], Davood Toghraie [a,*], Mohammad Hashemian [a], Farshid Aghadavoudi [a], Mohammad Akbari [b]

[a] Department of Mechanical Engineering, Khomeinishahr Branch, Islamic Azad University, Khomeinishahr, Iran
[b] Department of Mechanical Engineering, Najafabad Branch, Islamic Azad University, Najafabad, Iran

ARTICLE INFO

Keywords:
Molecular dynamics simulation
Nanofluid
Microchannel
Agglomeration
Electrical field

ABSTRACT

Recent progress in nanoparticle construction can be seen as a breakthrough in increasing heat transfer methods. The small size of particles and low volume fraction of particles leads to solving agglomeration and pressure drop problems and reduce the cost of storing and transporting nanofluids. Molecular dynamics simulation is one of the essential branches of computational physics that can predict various structures' atomic behavior. In this study, the effects of external electrostatic force and external electrical field on the density, velocity, temperature of atomic structures, and agglomeration of Fe_3O_4 nanoparticles in a copper microchannel are investigated. The results of the physical properties of this structure are estimated using molecular dynamics simulation and LAMMPS software. The results show that with increasing the applied external electrostatic force the maximum velocity is converged to 0.0071 Å /ps. Also, adding an external electrical field to the simulated nanofluid, the maximum values of density, velocity, and temperature are estimated to 1.32 g/cm^3, 0.0078 Å /ps, and 345 K, respectively. The external electrical field has a significant and essential role in the agglomeration process in atomic structures. Finally, it is observed that by increasing the external electrical field, the time required for the agglomeration process increases to 2.26 ns.

1. Introduction

Today, nanofluids are used in various fields [1–3]. The nanofluids application is divided into two parts: heat transfer and mass transfer [4–6]. Some exceptional properties like high stability, facile preparation, and acceptable viscosity have made nanofluids one of the most suitable and strong choices in both mass transfer and heat transfer fields. One of the basic needs in many industries and research projects is high-efficiency heat transfer [7–9]. Heat transfer environments are usually formed of fluids such as water, ethylene glycol, or oil. Compared to metals and even metal oxides, these fluids have a low thermal conductivity. Therefore, it is expected to show better thermal properties by adding nanoparticles to conventional fluids [10–13]. So far, most studies have focused on particles in millimeter or micrometer size. Particles on this scale cause severe problems in heat transfer equipment. These particles settle quickly in the system, and if the channel has a smaller diameter, the problem will be more serious. For instance, when flowing through microchannels, they cause agglomeration and clogging of the path and finally resulting in a large pressure drop. Also, the collision of these particles with each other and the system's walls leads to abrasion [14–16]. Recent progress in nanoparticle construction can be seen as a breakthrough in increasing heat transfer methods. The small size and low volume fraction of nanoparticles lead to solving agglomeration and pressure drop problems and reduce the cost of storing and transporting nanofluids [17–19]. In recent decades, molecular dynamics (MD) simulations have been used to study the properties of nanofluids. MD method is one of the essential branches of computational physics that can predict the atomic behavior of various structures [20,21]. Because molecular systems generally contain large numbers of particles, the properties of complex systems cannot be obtained analytically. But molecular dynamics simulation solves this problem by applying computational methods and thus creates an interface between laboratory results and theatricals [22–24].

In this computational study, the effect of external force and electrical

* Corresponding author.
E-mail address: Toghraee@iaukhsh.ac.ir (D. Toghraie).

https://doi.org/10.1016/j.icheatmasstransfer.2021.105182

Available online 7 February 2021

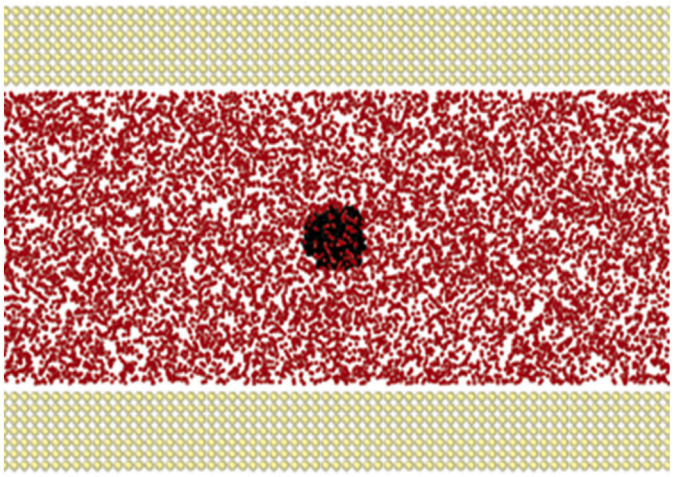

Fig. 1. Schematic of the atomic configuration of simulated water / Fe_3O_4 nanofluid.

field on factors such as temperature, density, velocity, and agglomeration process of water / Fe_3O_4 nanofluid flow in a microchannel has been investigated. The results are estimated using LAMMPS software [25,26] (published by Sandia National Laboratories (SNL)).

2. Computational method

To perform this simulation, at first ideal microchannels in micro-dimensions with 0.75 × 0.3 × 0.3 μm^3 is simulated at $T = 300$ K. The initial temperature is applied using the Nose-Hoover thermostat [27] to the simulated atomic structure. The walls of these microchannels are made of copper. The boundary conditions in the x and y-directions are considered periodic and the z-direction is considered constant. In the next step, Fe_3O_4 nanoparticles are added to the primary fluid and the system changes and flow in the microchannel are evaluated. Fig. 1 displays the atomic configuration of this structure (shown by Open Visualization Tool (OVITO) software) [28,29].

In this configuration, Fe_3O_4 nanoparticles are fixed in the middle of the microchannel. Then, by adding an external electrostatic force and an external electrical field to the nanofluid, the results are evaluated. From this approach, a new method can be designed to improve the behavior and the flow of nanofluids in microchannels. The foundation of molecular dynamics simulation is based on solving Newton's equation of motion (Newton's second law). By solving these equations, all particles' motion in the system in time scales can be simulated. In the formulation of this method, the force on the particle i can also be expressed as the gradient of the potential energy [30]:

$$F_i = -\nabla_i U \tag{1}$$

where F_i and U show the force exerted on the particle i and the system's potential energy, respectively. Newton's equation of motion can then relate the derivative of the potential function to the changes in position as a function of time. According to Newton's second law of motion, the relationship between motion and the applied force is calculated by Eq. (2) [30]:

$$F_i = m_i a_i = m_i \frac{d^2 r_i}{dt^2} \tag{2}$$

where m_i, a_i, and r_i show the mass (which is assumed to be independent of motion, velocity, and time) of particle *i*, acceleration of particle *i*, and motion of the particle i, respectively. Using the Verlet algorithm, the equation of motion in MD simulations can be calculated [31,32] as follows:

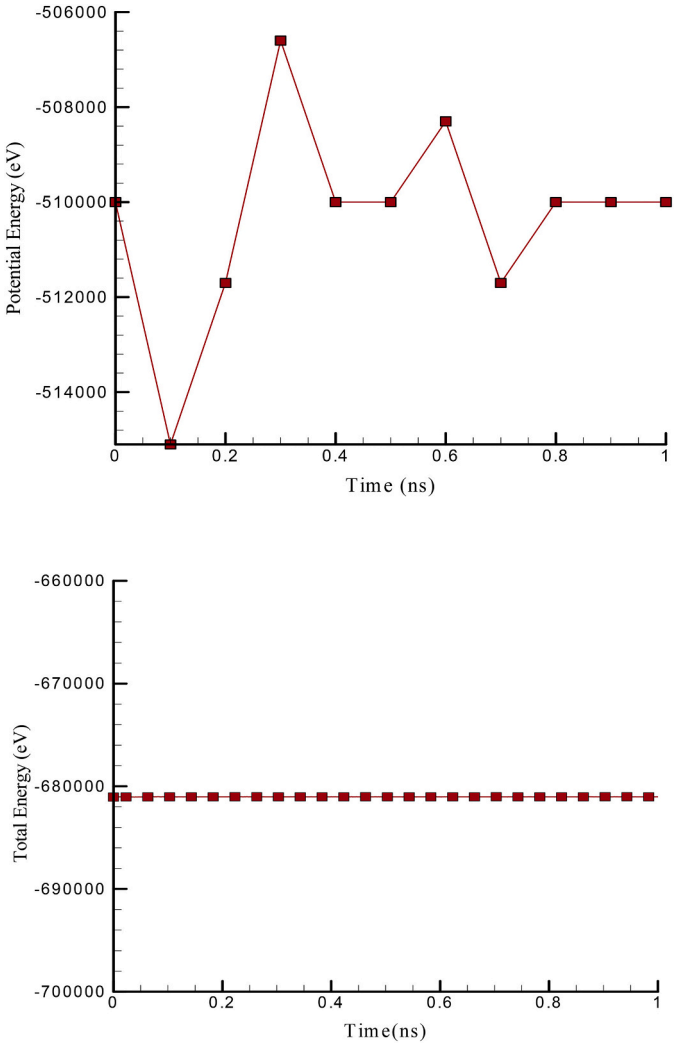

Fig. 2. Changes of potential energy and stability in the total energy of structure versus time.

$$r(t+\Delta t) = r(t) + v(t)\Delta t + \frac{1}{2}a(t)\Delta t^2 + O\left(\Delta t^4\right) \tag{3}$$

$$v(t+\Delta t) = v(t) + \frac{a(t)+a(t+\Delta t)}{2}\Delta t + O\left(\Delta t^2\right) \tag{4}$$

where v and Δt show the particle's velocity and the time interval (in femtoseconds). The Verlet algorithm uses positions (or velocity) and accelerations at time t to calculate new positions (or velocity) at time t+Δt.

Another essential factor in this simulation is the temperature. In classical physics, the temperature of atoms can be calculated using the following relation [33,34]:

$$\frac{1}{2}m|v|^2 = \frac{3}{2}k_b T \tag{5}$$

$$T(t) = \sum_i^N \frac{m_i v_i^2(t)}{k_b N} \tag{6}$$

where k_b and N shows the Boltzmann constant and degrees of freedom of the atomic system. The density and momentum of particles are given by [35]:

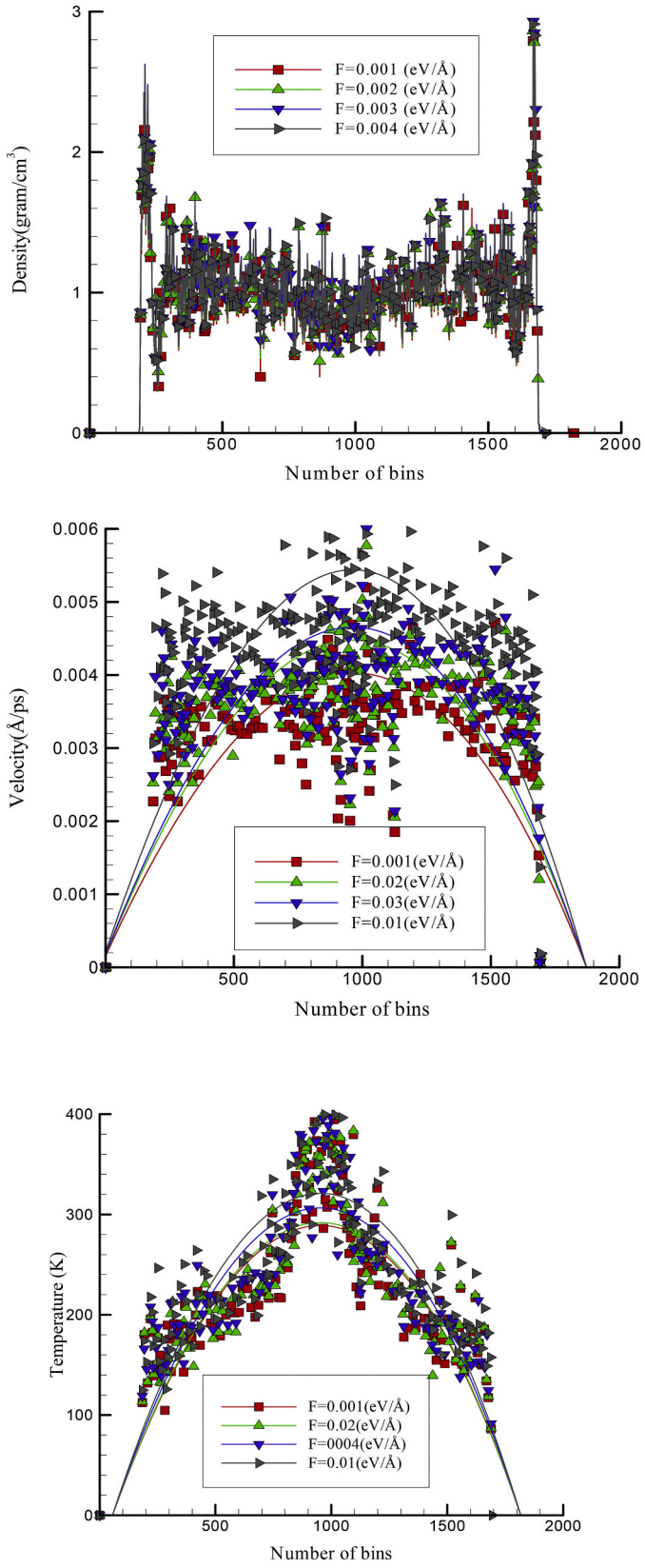

Fig. 3. Density, velocity, and temperature profiles of water / Fe_3O_4 nanofluid flow in the presence of applied variable external electrostatic force.

$$\rho = \frac{N}{V} \tag{7}$$

$$P_i = m_i v_i \tag{8}$$

In this simulation, the effect of the external force and electrical field on the Fe_3O_4 / water nanofluid is investigated. The following equation obtains the external electrostatic force [36]:

$$F = Eqcos(\omega t) \tag{9}$$

where E, q, and ω show the electrical field, electric charge, and frequency. The potential energy is a function of the atomic position (3 N) of all the atoms in the system. Due to this function's complicated nature, there is no analytical solution to the equations of motion; they must be solved numerically. In general, the sample's potential energy is obtained from the sum of the Leonard-Jones, EAM, and Columbus potential functions [37–39]. The Leonard-Jones potential function is a simple mathematical model that approximates the interactions between a pair of neutral particles and a molecule. The most common relation of the Leonard-Jones potential function is given by Eq. (10) [40,41]:

$$U_{LJ} = 4\varepsilon_{ij}\left[\left(\frac{\sigma_{ij}}{r_{ij}}\right)^{12} - \left(\frac{\sigma_{ij}}{r_{ij}}\right)^{6}\right] \tag{10}$$

where ε_{ij}, σ_{ij} and r_{ij} show the depth of the potential well, the distance at which the potential function becomes zero, and the distance of the particles from each other, respectively. The results show that by adding Fe_3O_4 nanoparticles to the base fluid (water), the amount of potential energy has a good convergence. This convergence in potential energy shows the presence of attraction and stability in total energy. Fig. 2 shows the changes in potential energy and the stability in the total energy of structure versus time (in 1 ns).

In the following, the effects of variable external electrostatic force and variable electrical field on the density, velocity, temperature, and the agglomeration of water / Fe_3O_4 nanofluid in a microchannel are investigated.

3. Results and discussion

3.1. The effects of applied external electrostatic force

An external electrostatic force applied to particles in a microchannel is one of the critical factors in the system's evolution. Therefore, in the first step, by adding variable external forces with magnitudes of 0.001, 0.002, 0.004, and 0.01 eV, the behavior of structure has been investigated. These studies are performed on physical quantities such as density, velocity, and temperature to investigate the nanofluid flow in a microchannel. Fig. 3 shows the changes in the density, velocity, and temperature in the presence of applied variable external electrostatic force.

As shown in Fig. 3, the density profile of simulated nanofluid does not change much across the microchannel. This is because the number of particles in the simulation box does not change. Increasing the applied external force has a positive correlation to the magnitude of the resultant force. Therefore, the acceleration of nanofluid particles is expected to be

Table 1
maximum values of density, velocity, and temperature of water / Fe_3O_4 nanofluid flow in the presence of applied variable external electrostatic force.

The magnitude of the external force (eV/ Å)	Maximum density (gr/cm^3)	Maximum velocity (Å /ps)	Maximum temperature (K)
0.001	1.41	0.0052	264
0.002	1.4	0.0058	276
0.004	1.39	0.0061	288
0.01	1.36	0.0071	308

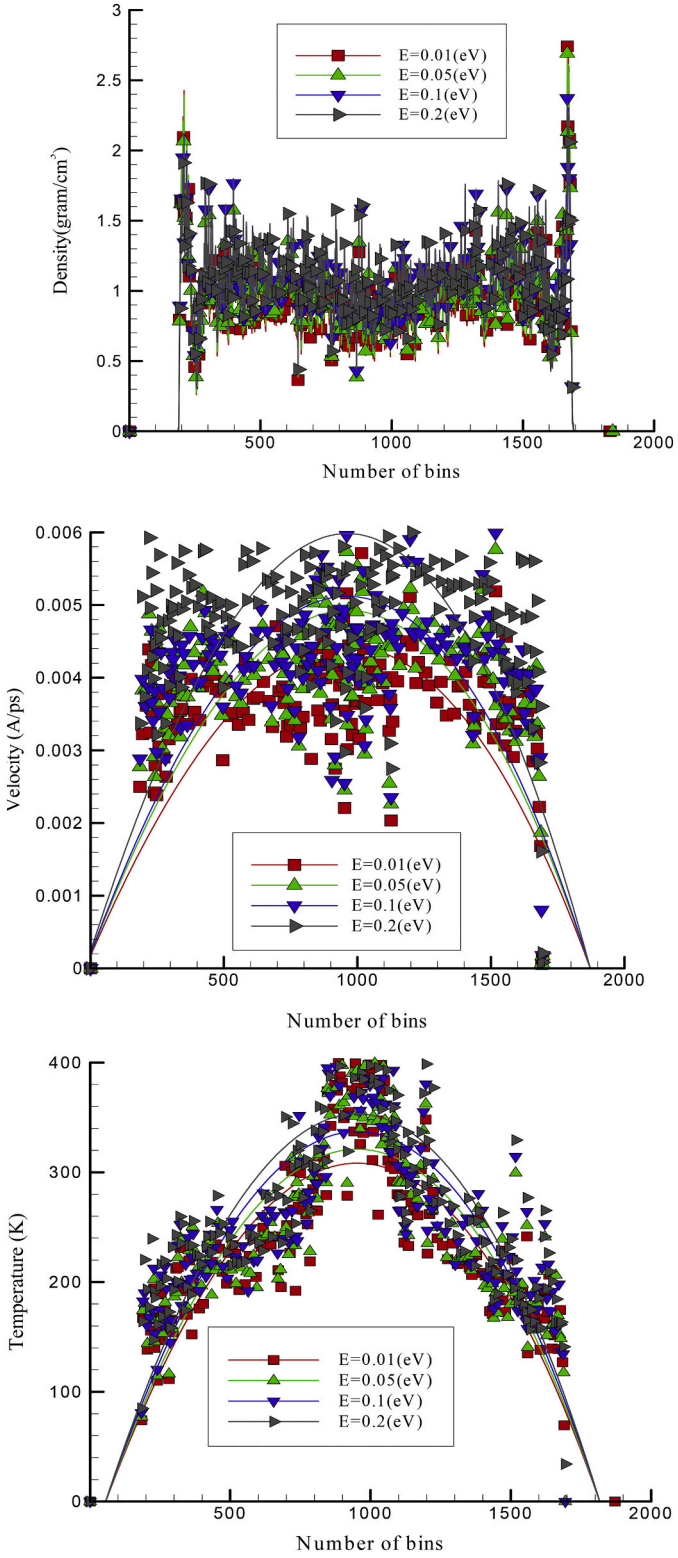

Fig. 4. Density, velocity, and temperature profiles of water / Fe_3O_4 nanofluid flow in the presence of an external electrical field.

a positive correlation to the external force. Finally, the amount of velocity increased. As shown in Fig. 3, as the amount of external electrostatic force increases or decreases, the Poiseuille flow [42] for the nanofluid is observed. As a result, the total motion of the particles does not change as the external force changes. Therefore, changing the applied external force leads to changing the kinetic energy, and finally, the simulated sample temperature also changes. The numerical values calculated are shown in Table 1.

Table 2
Maximum values of density, velocity, and temperature of water / Fe_3O_4 nanofluid flow in the presence of applied external electrical field.

The magnitude of the external electrical field (eV)	Maximum density (gr/cm^3)	Maximum velocity (Å /ps)	Maximum temperature (K)
0.01	1.4	0.0058	271
0.05	1.38	0.0064	301
0.1	1.35	0.0067	322
0. 2	1.32	0.0078	345

3.2. The effects of the applied external electrical field

An external electrical field is another factor influencing the behavior of nanofluid. In this part, by adding a variable external field with magnitudes of 0.01, 0.05, 0.01, and 0.01 eV, the electrophoretic behaviors of nanofluid flow have been investigated, because applying an external electrical field to a structure with an electric charge allows the study of the electroosmotic behavior [43,44]. Fig. 4 shows the changes in physical quantities of density, velocity, and temperature in the presence of an external electrical field.

According to Fig. 4, the increase in an external electric field applied to water / Fe_3O_4 nanofluid flow cannot change the density of nanofluid. Due to the predominance of interactions between microchannel walls and nanofluid particles, the density values do not change much with changing the external electrical field. The maximum values of this quantity can be seen on the boxes close to the microchannel walls. As a result, whatever the external electrical field increases, the amount of density in areas close to copper walls (microchannels) decreases. This is due to the greater acceleration of the particles in the presence of larger electrical fields. Therefore, increasing the external electrical field leads to increases in the velocity of the particles in the middle-boxes of the microchannel. Since the particles in the middle-boxes are less affected by the interactions of the wall particles, so the velocity changes of these particles are more than the nanofluid particles placed in the boxes next to the walls.

The velocity profile in Fig. 4 shows the increase in nanofluid velocity with increasing the external electrical field. Applied external electrical field leads to increases in the momentum of particles, and as a result, the motion of water / Fe_3O_4 particles increases. Also, changes in the motion of particles in atomic structures lead to temperature changes in the structure. The results show that increasing the external electrical field, the maximum temperature of nanofluid reaches to 345 K. On the other hand, according to Fig. 4, it can be said that the increase of the applied external electrical field does not cause deviate nanofluid from the Poiseuille flow. Also, parabolic diagrams for temperature profiles can be seen in this nanofluid. The maximum values of density, velocity, and temperature of the nanofluid flow in the variable external electrical field are reported in Table 2.

3.3. Investigation of the agglomeration process

Finally, agglomeration time in the nanofluid structure consists of two Fe_3O_4 nanoparticles in the presence of external electrostatic force with magnitudes among the amount of 0.001 to 0.01 eV / Å and external electrical fields with magnitudes of 0.01 to 0.2 eV have been investigated. According to physical concepts, the phenomenon of agglomeration is a destructive factor and researchers are trying to reduce or delay the amount of that. Computationally, the collision of two Fe_3O_4 nanoparticles in a copper microchannel happens after 1.47 ns and cause agglomeration of nanoparticles. This process is presented in Fig. 5. Increasing the external electrical field increases the agglomeration time

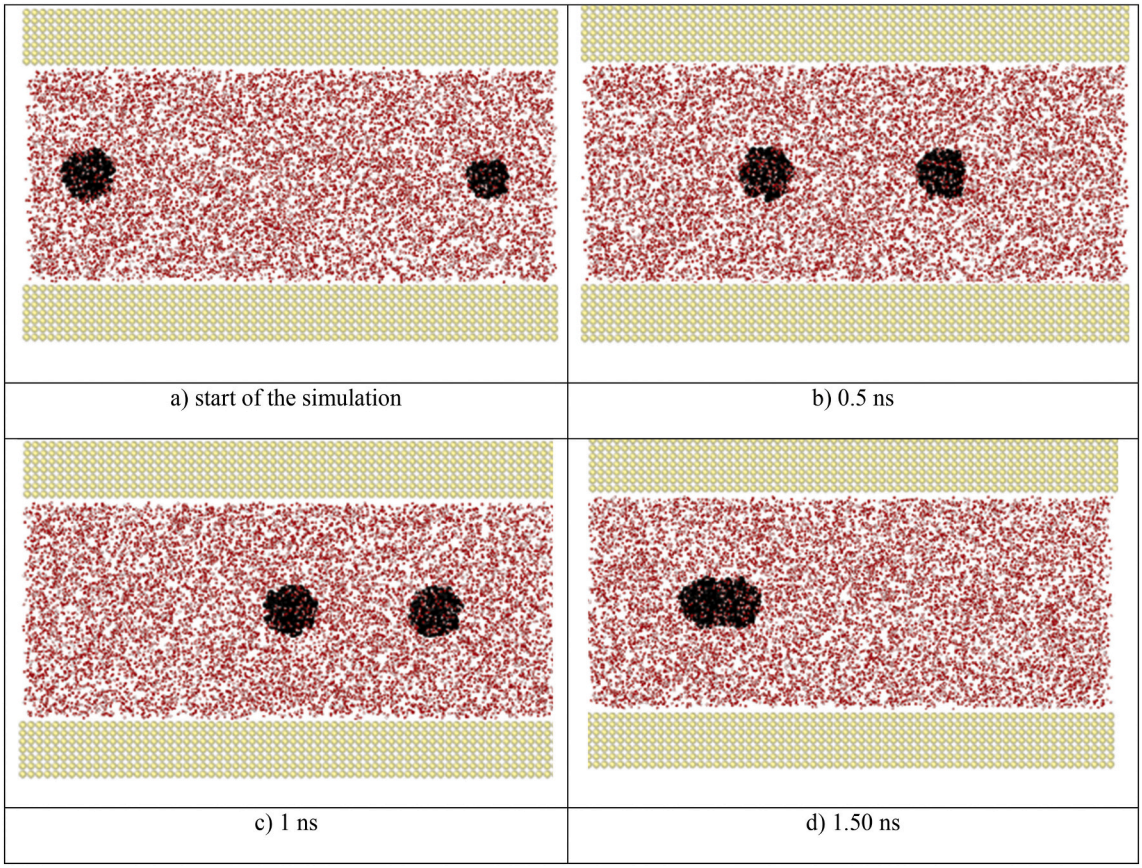

Fig. 5. Positions of Fe_3O_4 nanoparticles at different times.

Table 3
The agglomeration times of Fe_3O_4 nanoparticles in the presence of variable external electrostatic force and external electrical field.

Agglomeration time (ns)	The magnitude of the external force (eV/ Å)	Agglomeration time (ns)	The magnitude of the external electrical field (eV)
1.47	0.001	1.48	0.01
1.45	0.002	1.88	0.05
1.38	0.004	2.03	0.1
1.32	0.1	2.26	0.2

in the simulated nanoparticles. The results are reported in Table 3.

An external electrostatic force applied to the simulated nanofluid is another factor in the agglomeration of nanoparticles. The results show that by increasing the applied external force, the displacement of nanoparticles in the flow direction increases. So, these collisions occur in a shorter time. On a numerical scale, as the amount of applied external electrostatic force increases, the agglomeration process time decreases to 1.32 ns.

4. Conclusion

In this study, using computer simulations and molecular dynamics methods, the effects of applied external electrostatic force and electrical field on the nanofluid flow in a microchannel are investigated. The results are calculated by calculating the physical quantities such as density, velocity, temperature, and agglomeration phenomenon of the simulated fluid. The results are as follows:

- The increase in external electrostatic force applied to the nanofluid causes it to flow more freely. So, the maximum velocity of the nanofluid increases with increasing external force;
- Electroosmotic behavior in the nanofluid structure is observed by applying an external electrical field.
- Increases in the external electrical field lead to an increase in the maximum amount of velocity and temperature in a nanofluid.
- An external electrical field has played an effective and positive role in the agglomeration process in atomic structures. By adding this physical parameter, the agglomeration time in the simulation nanofluid increases.

Declaration of Competing Interest

The authors declare that they have no known competing financial interests or personal relationships that could have appeared to influence the work reported in this paper. Also, The authors declare that they did not employed by a government agency.

References

[1] M.U. Sajid, H.M. Ali, Recent advances in application of nanofluids in heat transfer devices: a critical review, Renew. Sust. Energ. Rev. 103 (2019) 556–592.
[2] T. Aguilar, et al., Investigation of enhanced thermal properties in NiO-based nanofluids for concentrating solar power applications: a molecular dynamics and experimental analysis, Appl. Energy 211 (2018) 677–688.
[3] S. Zeroual, H. Loulijat, E. Achehal, P. Estellé, A. Hasnaoui, S. Ouaskit, Viscosity of Ar-Cu nanofluids by molecular dynamics simulations: effects of nanoparticle content, temperature and potential interaction, J. Mol. Liq. 268 (2018) 490–496.
[4] P.S. Reddy, A.J. Chamkha, Heat and mass transfer characteristics of nanofluid over horizontal circular cylinder, Ain Shams Eng. J. 9 (4) (2018) 707–716.
[5] P.S. Reddy, P. Sreedevi, A.J. Chamkha, Magnetohydrodynamic (MHD) boundary layer heat and mass transfer characteristics of nanofluid over a vertical cone under convective boundary condition, Propul. Power Res. 7 (4) (2018) 308–319.

[6] P. Sudarsana Reddy, P. Sreedevi, Impact of chemical reaction and double stratification on heat and mass transfer characteristics of nanofluid flow over porous stretching sheet with thermal radiation, Int. J. Ambient Energy (2020) 1–11.
[7] M.R. Gholami, et al., The effect of rib shape on the behavior of laminar flow of oil/MWCNT nanofluid in a rectangular microchannel, J. Therm. Anal. Calorim. 134 (2018) 1611–1628.
[8] S.S. Sonawane, R.S. Khedkar, K.L. Wasewar, Effect of sonication time on enhancement of effective thermal conductivity of nano TiO2–water, ethylene glycol, and paraffin oil nanofluids and models comparisons, J. Exp. Nanosci. 10 (4) (2015) 310–322.
[9] W. Cui, Z. Shen, J. Yang, S. Wu, Rotation and migration of nanoparticles for heat transfer augmentation in nanofluids by molecular dynamics simulation, Case Stud. Therm. Eng. 6 (2015) 182–193.
[10] M. Farzinpour, D. Toghraie, B. Mehmandoust, F. Aghadavoudi, A. Karimipour, Molecular dynamics study of barrier effects on Ferro-nanofluid flow in the presence of constant and time-dependent external magnetic fields, J. Mol. Liq. 308 (2020), 113152.
[11] A.H. Saeedi, M. Akbari, D. Toghraie, An experimental study on rheological behavior of a nanofluid containing oxide nanoparticle and proposing a new correlation, Physica E 99 (2018) 285–293.
[12] D. Zhou, Heat transfer enhancement of copper nanofluid with acoustic cavitation, Int. J. Heat Mass Transf. 47 (14–16) (2004) 3109–3117.
[13] B. Farajollahi, S.G. Etemad, M. Hojjat, Heat transfer of nanofluids in a shell and tube heat exchanger, Int. J. Heat Mass Transf. 53 (1–3) (2010) 12–17.
[14] R. Hassandoost, S.R. Pouran, A. Khataee, Y. Orooji, S.W. Joo, Hierarchically structured ternary heterojunctions based on ce3+ / ce4+ modified Fe_3O_4 nanoparticles anchored onto graphene oxide sheets as magnetic visible-light-active photocatalysts for decontamination of oxytetracycline, J. Hazard. Mater. 376 (5) (2019) 200–211.
[15] H. Karimi-Maleh, B.G. Kumar, S. Rajendran, J.Q. Qin, S. Vadivel, D. Durgalakshmi, F. Gracia, M. Soto-Moscoso, Y. Orooji, F. Karimi, Tuning of metal oxides photocatalytic performance using Ag nanoparticles integration, J. Mol. Liq. 314 (2020), 113588.
[16] H. Karimi-Maleh, F. Karimi, Y. Orooji, G. Mansouri, A. Razmjou, A. Aygun, F. Sen, A new nickel-based co-crystal complex electrocatalyst amplified by NiO dope Pt nanostructure hybrid; a highly sensitive approach for determination of cysteamine in the presence of serotonin, Sci Rep. 10 (1) (2020), 11699.
[17] Y. Xuan, W. Roetzel, Conceptions for heat transfer correlation of nanofluids, Int. J. Heat Mass Transf. 43 (19) (2000) 3701–3707.
[18] K. Khanafer, K. Vafai, M. Lightstone, Buoyancy-driven heat transfer enhancement in a two-dimensional enclosure utilizing nanofluids, Int. J. Heat Mass Transf. 46 (19) (2003) 3639–3653.
[19] W. Daungthongsuk, S. Wongwises, A critical review of convective heat transfer of nanofluids, Renew. Sust. Energ. Rev. 11 (5) (2007) 797–817.
[20] A. Mosavi, M. Hekmatifar, A.a. Alizadeh, D. Toghraie, R. Sabetvand, A. Karimipour, The molecular dynamics simulation of thermal manner of Ar/Cu nanofluid flow: the effects of spherical barriers size, J. Mol. Liquids 319 (2020), 114183.
[21] M. Hekmatifar, et al., The study of asphaltene desorption from the iron surface with molecular dynamics method, J. Mol. Liq. 318 (2020), 114325.
[22] M. Hekmatifar, D. Toghraie, B. Mehmandoust, F. Aghadavoudi, S.A. Eftekhari, Molecular dynamics simulation of the phase transition process in the atomic scale for Ar/Cu nanofluid on the platinum plates, Int. Commun. Heat Mass Transf. 117 (2020), 104798.
[23] S.A. Adcock, J.A. McCammon, Molecular dynamics: survey of methods for simulating the activity of proteins, Chem. Rev. 106 (5) (2006) 1589–1615.
[24] A. Hospital, J.R. Goñi, M. Orozco, J.L. Gelpí, Molecular dynamics simulations: advances and applications, Adv. Appl. Bioinform. Chem. 8 (2015) 37.
[25] K.D. Hammond, Parallel point defect identification in molecular dynamics simulations without post-processing: a compute and dump style for LAMMPS, Comput. Phys. Commun. 247 (2020), 106862.
[26] W.M. Brown, J.-M.Y. Carrillo, N. Gavhane, F.M. Thakkar, S.J. Plimpton, Optimizing legacy molecular dynamics software with directive-based offload, Comput. Phys. Commun. 195 (2015) 95–101.
[27] D.J. Evans, B.L. Holian, The nose–hoover thermostat, J. Chem. Phys. 83 (8) (1985) 4069–4074.
[28] A. Stukowski, Visualization and analysis of atomistic simulation data with OVITO–the Open Visualization Tool, Model. Simul. Mater. Sci. Eng. 18 (1) (2009), 015012.
[29] A. Stukowski, Visualization and analysis strategies for atomistic simulations, in: Multiscale Materials Modeling for Nanomechanics, Springer, 2016, pp. 317–336.
[30] D.C. Rapaport, The Art of Molecular Dynamics Simulation, Cambridge University Press, 2004.
[31] Q. Spreiter, M. Walter, Classical molecular dynamics simulation with the Velocity Verlet algorithm at strong external magnetic fields, J. Comput. Phys. 152 (1) (1999) 102–119.
[32] R.E. Gillilan, K.R. Wilson, Shadowing, rare events, and rubber bands. A variational Verlet algorithm for molecular dynamics, J. Chem. Phys. 97 (3) (1992) 1757–1772.
[33] R.B. Dehkordi, D. Toghraie, M. Hashemian, F. Aghadavoudi, M. Akbari, Molecular dynamics simulation of ferro-nanofluid flow in a microchannel in the presence of external electrical field: effects of Fe3O4 nanoparticles, Int. Commun. Heat Mass Transf. 116 (2020), 104653.
[34] B. Lane, et al., Nanobots and Europa, teaching nanotechnology via futuristic space exploration, Chem. Educ. 16 (1) (2011) 91–98.
[35] M.P. Allen, D. Frenkel, J. Talbot, Molecular dynamics simulation using hard particles, Comput. Phys. Rep. 9 (6) (1989) 301–353.
[36] D.H. Jung, J.H. Yang, M.S. Jhon, The effect of an external electrical field on the structure of liquid water using molecular dynamics simulations, Chem. Phys. 244 (2–3) (1999) 331–337.
[37] M.R. Fellinger, First Principles-based Interatomic Potentials for Modeling the Body-centered Cubic Metals V, Nb, Ta, Mo, and W, The Ohio State University, 2013.
[38] J. Li, Basic molecular dynamics, in: Handbook of Materials Modeling, Springer, 2005, pp. 565–588.
[39] H. Rafii-Tabar, G.A. Mansoori, Interatomic Potential Models for Nanostructures, arXiv preprint, 2018. arXiv:1806.06291.
[40] A. Oluwajobi, X. Chen, The effect of interatomic potentials on the molecular dynamics simulation of nanometric machining, Int. J. Autom. Comput. 8 (3) (2011) 326.
[41] N. Von Solms, R. O'lenick, Y. Chiew, Leonard-Jones chain mixtures: variational theory and Monte Carlo simulation results, Mol. Phys. 96 (1) (1999) 15–29.
[42] M.B. Motlagh, M. Kalteh, Simulating the convective heat transfer of nanofluid Poiseuille flow in a nanochannel by molecular dynamics method, Int. Commun. Heat Mass Transf. 111 (2020), 104478.
[43] N. Ali, J.A. Teixeira, A. Addali, A review on nanofluids: fabrication, stability, and thermophysical properties, J. Nanomater. 2018 (2018).
[44] H. Kamiya, et al., Characteristics and behavior of nanoparticles and its dispersion systems, in: Nanoparticle Technology Handbook, Elsevier, 2008, pp. 113–176.